

Carbon Dioxide as a C₁ Building Block. Mechanism of Palladium-Catalyzed Carboxylation of Aromatic Halides

Christian Amatore,* Anny Jutand,* Fouad Khalil, and Merete F. Nielsen†

Ecole Normale Supérieure, Département de Chimie, URA CNRS 1110, 24 rue Lhomond, 75231 Paris Cedex 05, France. Received December 18, 1991

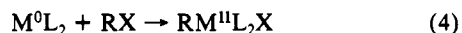
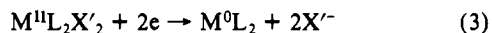
Abstract: The reduction of aryl halides in the presence of stoichiometric amounts of carbon dioxide and catalytic amounts of Pd^{II}Cl₂(PPh₃)₂ has been previously reported to result in the formation of the corresponding carboxylic acids. It is shown here that the mechanism proceeds via a catalytic cycle initiated by the one-step, two-electron reduction of the divalent palladium complex followed by oxidative addition of the aryl halide to the resulting poorly ligated zerovalent palladium center "Pd⁰(PPh₃)₂", to afford the corresponding σ -aryl palladium(II) intermediate. One-step, two-electron reduction of the latter yields an anionic σ -aryl palladium(0), ArPd⁰(PPh₃)₂⁻, which reversibly dissociates to restore the low-ligated zerovalent palladium complex, "Pd⁰(PPh₃)₂", while producing a free σ -aryl anion, Ar⁻. Nucleophilic attack of carbon dioxide by the latter yields the carboxylate derivative, ArCO₂⁻, while oxidative addition of the aryl halide to "Pd⁰(PPh₃)₂" completes the catalytic cycle. It is thus concluded that the palladium-catalyzed carboxylation proceeds only through the involvement of diamagnetic palladium-centered intermediates, in contradiction with what has been established previously for the nickel catalysis of the same reaction.

Introduction

Several approaches exist by which carbon dioxide can be activated to be used as a C₁ building block in organic chemistry.¹⁻⁵ One of the most simple, at least conceptually, consists of the carboxylation of an organic substrate by means of a pseudo Grignard reaction. Thus an organic halide or pseudo-halide can be reduced to the corresponding anion^{3a,c,d,f,g,j,m,n} (or an unsaturated organic material reduced to its anion radical^{4,5}), which then nucleophilically adds to carbon dioxide, resulting in carbon-carbon bond formation:

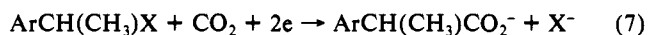


However, the main drawback of these approaches is the high reactivity of the corresponding anions or anion radicals, which may undergo several competing reactions, protonation leading to an overall reductive hydrogenation of the organic substrate being one of them.⁶ A second difficulty is that they require the organic substrate to be reducible before CO₂, which may be impossible for situations of synthetic interest, where the organic moiety is not activated by the presence of electrophores or extended orbital delocalization. To bypass both difficulties several groups have examined the possibility of using transition metal complexes to catalyze the organic halide reduction in eq 1.^{3b,e,h,i,k,l,o-q} Thus a zerovalent transition metal can be generated, e.g., by reduction of one of its divalent precursors, at a potential much less negative than that of the organic substrate or of carbon dioxide; oxidative addition of the organic halide to the zerovalent metal center affords a divalent organometallic species, prone to react with carbon dioxide after its activation by electron transfer:^{3p,q}



This presents an obvious advantage over the direct reduction in eq 1, since the above process allows the reductive activation of an organic substrate at a potential generally less negative than that of its direct reduction. Several groups have taken advantage of this property for proposing nickel- or palladium-mediated

electrocarboxylations of aromatic or benzylic halides:^{3b,e,h,i,k,l,o-q}



It is noteworthy that these preparative processes are catalytic

(1) For reviews on carbon dioxide activation by metal complexes, see, e.g.: (a) Darenbourg, D. J.; Kudarowski, R. A. *Adv. Organomet. Chem.* **1983**, *22*, 129. (b) Behr, A. *Angew. Chem., Int. Ed. Engl.* **1988**, *27*, 661. (c) Braustein, P.; Matt, D.; Nobel, D. *Chem. Rev.* **1988**, *88*, 747.

(2) For documented reviews on the electrochemical activation of carbon dioxide, see ref 1 and the following: (a) Silvestri, G. In *Carbon Dioxide as a Source of Carbon*; Aresta, M., Forti, G., Eds.; NATO Advanced Study Institute Series C; Reidel: Dordrecht, 1987; pp 339-369. (b) Silvestri, G.; Gambino, S.; Filardo, G. In *Enzymatic Model Carboxylation Reduction Reactions and Carbon Dioxide Utilization*; NATO Advanced Study Institute Series C; Reidel: Dordrecht, 1990; Vol. 314, pp 101-127.

(3) For electrocarboxylation of organic halides or pseudo-halides, see: (a) Baizer, M. M.; Chruma, J. L. *J. Org. Chem.* **1972**, *37*, 1951. (b) Troupel, M.; Rollin, Y.; Perichon, J.; Fauvarque, J. F. *New J. Chem.* **1981**, *5*, 26. (c) Fuchs, P.; Hess, U.; Holst, H. H.; Lund, H. *Acta Chem. Scand., Ser. B* **1981**, *35*, 185. (d) Barba, F.; Guirado, A.; Zapata, A. *Electrochim. Acta* **1982**, *27*, 1335. (e) Fauvarque, J. F.; Chevrot, C.; Jutand, A.; François, M.; Perichon, J. *J. Organomet. Chem.* **1984**, *264*, 273. (f) Ruettinger, H. H.; Rudolf, W. D.; Matschiner, H. *Electrochim. Acta* **1985**, *30*, 155. (g) Sock, O.; Troupel, M.; Perichon, J. *Tetrahedron Lett.* **1985**, *26*, 1509. (h) Torii, S.; Tanaka, H.; Hamatani, T.; Morisaki, K.; Jutand, A.; Pflüger, F.; Fauvarque, J. F. *Chem. Lett.* **1986**, 169. (i) Fauvarque, J. F.; Jutand, A.; François, M. *New J. Chem.* **1986**, *10*, 119. (j) Koch, D. A.; Henne, B. J.; Bartak, D. E. *J. Electrochem. Soc.* **1987**, *134*, 3062. (k) Fauvarque, J. F.; Jutand, A.; François, M. *J. Appl. Electrochem.* **1988**, *18*, 109. (l) Fauvarque, J. F.; Jutand, A.; François, M.; Petit, M. A. *J. Appl. Electrochem.* **1988**, *18*, 116. (m) Heintz, M.; Sock, O.; Saboureaux, C.; Perichon, J.; Troupel, M. *Tetrahedron* **1988**, *44*, 1631. (n) Maran, F.; Fabrizio, M.; D'Angeli, F.; Vianello, E. *Tetrahedron* **1988**, *44*, 2351. (o) Fauvarque, J. F.; de Zelicourt, Y.; Amatore, C.; Jutand, A. *J. Appl. Electrochem.* **1990**, *20*, 338. (p) Amatore, C.; Jutand, A. *J. Am. Chem. Soc.* **1991**, *113*, 2819. (q) Amatore, C.; Jutand, A. *J. Electroanal. Chem. Interfacial Electrochem.* **1991**, *306*, 141.

(4) For electrocarboxylation of unsaturated hydrocarbons, see: (a) Wawzonek, S.; Wearing, D. *J. Am. Chem. Soc.* **1959**, *81*, 2067. (b) Tkatchenko, I. B. M.; Ballivet-Tkatchenko, D. A.; El Murr, N.; Tanji, J.; Payne, J. D. French Patent 2542764, 1984; *Chem. Abstr.* **1985**, *102*, 069341. (c) Pletcher, D.; Girault, J. *J. Appl. Electrochem.* **1986**, *16*, 791. (d) Daniele, S.; Ugo, P.; Bontempelli, G.; Fiorani, M. *J. Electroanal. Chem. Interfacial Electrochem.* **1987**, *219*, 259. (e) Gambino, S.; Gennaro, A.; Filardo, G.; Silvestri, G.; Vianello, E. *J. Electrochem. Soc.* **1987**, *134*, 2172. (f) Schultz von Itter, N.; Steckhan, E. *Tetrahedron* **1987**, *43*, 2475. (g) Dunach, E.; Perichon, J. *J. Organomet. Chem.* **1988**, *352*, 239. (h) Labbe, E.; Dunach, E.; Perichon, J. *J. Organomet. Chem.* **1988**, *353*, C51. (i) Dunach, E.; Derien, S.; Perichon, J. *J. Organomet. Chem.* **1989**, *364*, C33. (j) Derien, S.; Dunach, E.; Perichon, J. *J. Am. Chem. Soc.* **1991**, *113*, 8447.

* To whom any correspondence should be addressed.

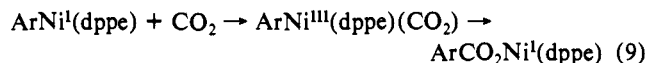
† Present address: Department of General and Organic Chemistry, the H. C. Ørsted Institute, Universitetsparken 5, DK-2100 Copenhagen Ø, Denmark.

in transition metals. This establishes that the zerovalent transition metal undergoing oxidative addition in eq 4 must be regenerated by a succession of steps following the initial reduction of $\text{RM}^{\text{II}}\text{L}_2\text{X}$ in eq 5.^{3p,q,7} The exact nature of the reactions initiated by this reduction step appears then to be essential for the regeneration of the catalyst. Moreover, this sequence also governs the activation of the organic moiety and therefore its reactivity vs any electrophile, e.g., CO_2 .

In a previous work^{3p,q} we have shown that the catalysis of the electrocarboxylation of aromatic halides by $\text{NiCl}_2(\text{dppe})$, $\text{dppe} = \text{Ph}_2\text{P}(\text{CH}_2)_2\text{PPh}_2$, occurred via the process in eqs 3 and 4, followed by the one-electron reduction of the insertion complex $\text{ArNi}^{\text{II}}(\text{dppe})\text{X}$ to afford a paramagnetic nickel(I) species,



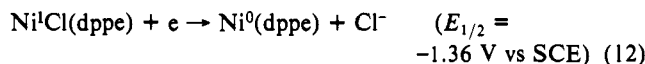
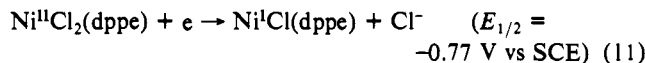
which further reacted with carbon dioxide, via a two-step mechanism, to afford a nickel(I) arenecarboxylate:



One-electron reduction of the latter gave eventually the desired arenecarboxylate and regenerated the zerovalent nickel catalyst:



This example suffices to demonstrate that the catalysis of the sequence in eqs 1 and 2 may not necessarily proceed via a Grignard analog, i.e., of an aryl anion stabilized by coordination to a transition metal center, but may as well involve paramagnetic intermediates (eq 9).⁸ This result is to be paralleled with the fact that all the divalent nickel precursors of $\text{Ni}^0(\text{dppe})$, e.g., $\text{Ni}^{\text{II}}\text{Cl}_2(\text{dppe})$, also undergo a reduction in two one-electron steps.^{7,8d}



rather than an overall two-electron reduction as depicted in eq 3. This two-step reduction is not characteristic of nickel(II)-centered complexes since, for example, replacement of the dppe ligand by bipyridine⁹ or by two monodentate phosphine ligands results in the observation of an overall two-electron reduction wave.¹⁰

Such a dichotomy, viz., a one-electron vs one overall two-electron reduction, exists also for the analogous palladium(II) complexes, $\text{Pd}^{\text{II}}\text{Cl}_2\text{P}_2$, where P is a phosphorus-centered ligand. When P_2 consists of two monodentate phosphines, i.e., $\text{P} =$

(5) For electrocarboxylation of carbonyl compounds, see: (a) Le Moing, O. A.; Delaunay, J.; Lebourg, A.; Simonet, J. *Tetrahedron* **1985**, *41*, 4483. (b) Silvestri, G.; Gambino, S.; Filardo, G. *Tetrahedron Lett.* **1986**, *27*, 3429. (c) Wagenknecht, J. H. U.S. Patent 4582577, 1986; *Chem. Abstr.* **1986**, *105*, 050861; U.S. Patent 4601797, 1986; *Chem. Abstr.* **1987**, *106*, 024982. (d) Bulhoes, L. O. de Sousa, Zara, A. J. *J. Electroanal. Chem. Interfacial Electrochem.* **1988**, *248*, 159. (e) Di Lorenzo, S.; Silvestri, G.; Gambino, S.; Filardo, G. *Chem. Eng. J. (Lausanne)* **1989**, *40*, 187. For electrocarboxylation of imines, see: (f) Komenda, J.; Hess, U. *Z. Phys. Chem. (Leipzig)* **1984**, *265*, 17. (g) Komenda, J.; Fiala, R.; Hess, U. *Z. Phys. Chem. (Leipzig)* **1987**, *268*, 48. (h) Hess, U.; Blumke, C. O. *Z. Chem.* **1988**, *28*, 144. (i) Hess, U.; Granitza, D.; Thiele, R. *Z. Chem.* **1988**, *28*, 188. (j) Silvestri, G.; Gambino, S.; Filardo, G. *Gazz. Chim. Ital.* **1988**, *118*, 643.

(6) See, for example: Weinberg, N. L. In *Technique of Electroorganic Synthesis*; Wiley Interscience: New York, 1975; Part II, p 189 and refs 3c, d, and g.

(7) (a) Amatore, C.; Jutand, A. *Organometallics* **1988**, *7*, 2203. (b) Amatore, C.; Jutand, A.; Mottier, L. *J. Electroanal. Chem. Interfacial Electrochem.* **1991**, *306*, 125.

(8) Compare refs 7 and the following: (a) Tsou, T. T.; Kochi, J. K. *J. Am. Chem. Soc.* **1979**, *101*, 7547. (b) Tsou, T. T.; Kochi, J. K. *J. Org. Chem.* **1980**, *45*, 1930. (c) Colon, I.; Kelsey, D. R. *J. Org. Chem.* **1986**, *51*, 2627. (d) Fox, M. A.; Chandler, D. A.; Lee, C. *J. Org. Chem.* **1991**, *56*, 3246.

(9) Amatore, C.; Azzabi, M.; Calas, P.; Jutand, A.; Lefrou, C.; Rollin, Y. *J. Electroanal. Chem. Interfacial Electrochem.* **1990**, *288*, 45.

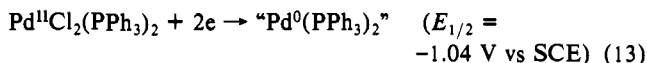
(10) Troupel, M.; Rollin, Y.; Sibille, S.; Fauvarque, J. F.; Perichon, J. *J. Chem. Res., Synop.* **1980**, *5*, 26.

Table I. Preparative Scale Electrolysis of $p\text{-ZC}_6\text{H}_4\text{Pd}^{\text{II}}\text{XP}_2$ (0.5 mmol), in the Presence of Saturated Carbon Dioxide (0.205 M^{13}), in THF (50 mL), with 0.3 M NBu_4BF_4 , at 20 °C

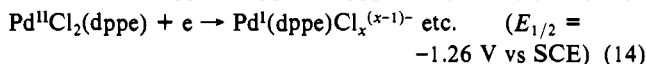
$p\text{-ZC}_6\text{H}_4\text{Pd}^{\text{II}}\text{XP}_2$			electrolysis potential (V vs SCE)	F/mol	yield (%) ^a (ArCO ₂ H)
Z	P ₂	X			
H	dppe	Br	-1.80	2.0	80
H	(PPh ₃) ₂	Br	-2.25	2.5	74
CH ₃ ^b	(PPh ₃) ₂	I	-2.00	2.2	98
CH ₃ CO	(PPh ₃) ₂	Br	-2.25	2.5	66 ^b
CN ^c	(PPh ₃) ₂	Br	-1.70	1.6 ^d	56 ^e

^a Isolated yields, defined vs the initial starting material. ^b 20% of dimer ($\text{CH}_3\text{COC}_6\text{H}_4$)₂ was isolated. ^c Synthesized in situ by the stoichiometric reaction of $\text{Pd}^0(\text{PPh}_3)_4$ with $p\text{-ZC}_6\text{H}_4\text{X}$, prior to electrolysis. ^d Electrolysis was interrupted after 75% conversion of the initial starting material. ^e Isolated as p -terephthalic acid.

PPh_3 ,^{9,11,12a} PBu_3 ,^{12a} etc., reduction of $\text{Pd}^{\text{II}}\text{Cl}_2\text{P}_2$ occurs via a single two-electron wave, e.g.,



whereas it proceeds via a one-electron wave when P_2 is a bidentate ligand such as dppe or dppp ,^{12a} $\text{dppp} = \text{Ph}_2\text{P}(\text{CH}_2)_3\text{PPh}_2$, e.g.:



Interestingly, this dichotomy is again paralleled by that observed for the reduction of the corresponding (σ -aryl)palladium(II) derivatives. For example, $\text{C}_6\text{H}_5\text{Pd}^{\text{II}}(\text{PPh}_3)_2$ undergoes an overall two-electron^{12b} reduction at $E^p = -1.98 \text{ V vs SCE}$ at $0.2 \text{ V}\cdot\text{s}^{-1}$ (vide infra), whereas $\text{C}_6\text{H}_5\text{Pd}^{\text{II}}(\text{dppe})$ is reduced via a one-electron^{12b} process ($E^p = -1.79 \text{ V vs SCE}$ at $0.2 \text{ V}\cdot\text{s}^{-1}$). It is noteworthy that $\text{Pd}^{\text{II}}\text{Cl}_2(\text{PPh}_3)_2$ is an active catalyst in electrocarboxylations^{3h} whereas, in contradiction with the case of nickel (eqs 8–10), $\text{Pd}^{\text{II}}\text{Cl}_2(\text{dppe})$ is inactive as a catalyst, although the reduction of $\text{C}_6\text{H}_5\text{Pd}^{\text{II}}\text{Br}(\text{dppe})$ in the presence of carbon dioxide affords a good yield of benzoic acid (see Table I and ref 3h).

What precedes clearly establishes that, despite an apparent unity, at least two main mechanistic classes must be considered so as to rationalize the catalytic behavior of transition metal complexes in electrocarboxylation of organic halides (eqs 6 and 7). The first class involves those systems that require a one-electron activation of the intermediate (σ -aryl)metal derivative formed by oxidative addition of the organic halide to the zerovalent metal complex produced via a two-step reduction of the divalent precursor $\text{M}^{\text{II}}\text{X}_2\text{L}_2$. In this class, whose paragon is $\text{Ni}^{\text{II}}\text{Cl}_2(\text{dppe})$, catalysis proceeds by a succession of chemical and electron-transfer steps involving paramagnetic intermediates, as recalled above (eqs 8–10).^{3p,q} The second class, much less understood at this stage, corresponds to a one-step, two-electron activation of the intermediate (σ -aryl)metal derivative formed by oxidative addition of the organic halide to the zerovalent metal complex, this latter species being now produced via a one-step overall two-electron reduction of the divalent precursor $\text{M}^{\text{II}}\text{X}_2\text{L}_2$. On the basis of our present knowledge, this second class appears to be the exclusive class effective for systems involving palladium-centered catalysts and is best represented by $\text{Pd}^{\text{II}}\text{Cl}_2(\text{PPh}_3)_2$. Although several preparative processes using this catalyst, including electrocarboxylation of aromatic halides,^{3h} have been reported, the

(11) (a) Amatore, C.; Azzabi, M.; Jutand, A. *J. Am. Chem. Soc.* **1991**, *113*, 1670. (b) Amatore, C.; Azzabi, M.; Jutand, A. *J. Am. Chem. Soc.* **1991**, *113*, 8375.

(12) (a) The absolute overall electron stoichiometries for the electrochemical reductions of $\text{Pd}^{\text{II}}\text{Cl}_2\text{P}_2$ were determined to be as follows: $n = 2.04 \pm 0.15$ ($\text{P}_2 = (\text{PPh}_3)_2$ in THF),^{9,11} $n = 1.90 \pm 0.20$ ($\text{P}_2 = (\text{PBu}_3)_2$ in DMF), $n = 1.11 \pm 0.12$ ($\text{P}_2 = \text{dppe} = \text{Ph}_2\text{P}(\text{CH}_2)_2\text{PPh}_2$ in THF), $n = 1.20 \pm 0.11$ ($\text{P}_2 = \text{dppp} = \text{Ph}_2\text{P}(\text{CH}_2)_3\text{PPh}_2$ in THF). The determinations were carried out by the combined use of steady-state voltammetry at a gold disk ultramicroelectrode (25- μm diameter) and transient chronoamperometry at gold disk microelectrodes (0.5–0.125-mm diameter) according to the procedure described in ref 9. For all determinations ferrocene was used as an internal standard (see ref 9). (b) $n = 0.95 \pm 0.20$ and $n = 1.9 \pm 0.15$ were determined in THF for $\text{C}_6\text{H}_5\text{Pd}^{\text{II}}(\text{dppe})$ and $\text{C}_6\text{H}_5\text{Pd}^{\text{II}}(\text{PPh}_3)_2$, respectively, according to the same procedure, with ferrocene as an internal standard.

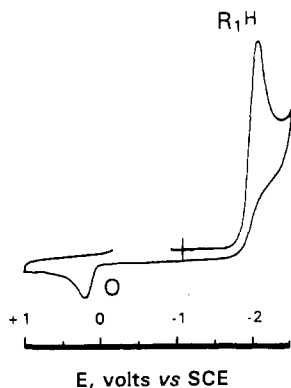
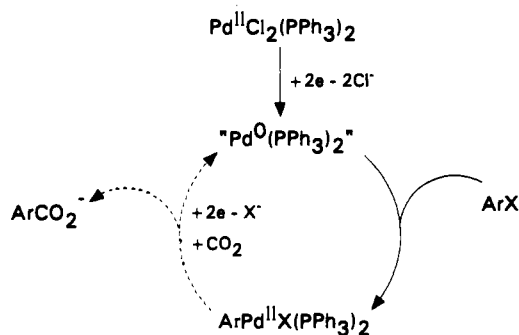


Figure 1. Cyclic voltammogram of $C_6H_5Pd^{II}Cl(PPh_3)_2$, 2 mM, in THF, with 0.3 M NBu_4BF_4 , at a gold disk electrode (i.d. 0.5 mm), in the presence of CO_2 , 5 mM. Scan rate $0.2 V \cdot s^{-1}$. At $20^\circ C$.

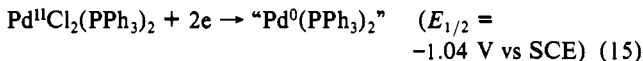
Scheme I



corresponding catalytic mechanisms remain unknown. It is the purpose of the work hereafter to cast some understanding on this mechanism, particularly for what concerns its crucial step(s), viz., the reaction(s) initiated by the two-electron activation of the (σ -aryl)palladium(II) intermediate.

Results

General Outline of the Catalytic Sequence. In the presence of catalytic amounts (10%) of $Pd^{II}Cl_2(PPh_3)_2$ and saturated carbon dioxide, the reduction of aromatic halides affords high yields of arenecarboxylate.^{3h} Whenever the potential is set at the potential of the reduction wave of $Pd^{II}Cl_2(PPh_3)_2$, one observes only a net consumption of two electrons per $Pd^{II}Cl_2(PPh_3)_2$, with the quantitative formation of the (σ -aryl)palladium(II) derivative:^{11b}



This suggests that the latter species must necessarily be reduced for the electrocarboxylation to proceed. This is further confirmed by the fact that the electrolysis of authentic samples of $p-ZC_6H_4Pd^{II}X(PPh_3)_2$ in the presence of saturated carbon dioxide (ca. 0.2 M in THF)¹³ affords the corresponding arenecarboxylates, as shown in Table I, in complete agreement with the results presented in ref 3h.¹⁴

(13) The concentration of saturated carbon dioxide in THF has been reported to be 0.205 M, under very similar conditions (viz., $T = 25^\circ C$ instead of $20^\circ C$ as used in this study). See: Gennaro, A.; Isse, A. A.; Vianello, E. *J. Electroanal. Chem. Interfacial Electrochem.* **1990**, *289*, 203.

(14) (a) The close agreement between the results reported in ref 3h and those in Table I is as expected since, irrespective of their galvanostatic (ref 3h) or potentiostatic control (Table I), the electrolysis proceeds in both cases at the reduction potential of the (σ -aryl)palladium(II) derivative, which is the starting material under our conditions or that is constantly regenerated by oxidative addition (eq 16) of the aryl halide to the zerovalent palladium catalyst under the conditions of ref 3h. (b) One observes nevertheless that under our conditions almost no aromatic derivative ArH is formed, whereas significant yields of the latter are reported in ref 3h. This discrepancy may be rationalized (vide infra) by observing that the proticity of the medium is certainly much lower under our experimental conditions (anhydrous THF vs DMF in ref 3h).

Table II. Cyclic Voltammetry Data for $p-ZC_6H_4Pd^{II}X(PPh_3)_2$, 2 mM, in THF, with 0.3 M NBu_4BF_4 , at a Gold Disk Electrode (i.d. 0.125 mm). Peak Potentials of Waves R_1^z , O^z , and O at $10 V \cdot s^{-1}$, in V vs SCE, at $20^\circ C$

$p-ZC_6H_4Pd^{II}X(PPh_3)_2$		$E_{R_1^z}^p$	$E_{O^z}^p$	E_O^p
Z	X			
H	Cl	-2.12	-0.53	0.19
H	Br	-2.10	-0.53	0.18
H	I	-2.02	-0.53	0.19
CH ₃	I	-2.04	-0.55	0.17
CH ₃ CO	Br	-2.01	-0.49	0.19
		-2.57 ^a	-0.69 ^b	
CN	Br	-1.92	-0.46	0.19
		-2.36 ^c		

^a Wave $R_3^{CH_3CO}$. ^b Wave O^{*CH_3CO} . ^c Wave R_2^{CN} .

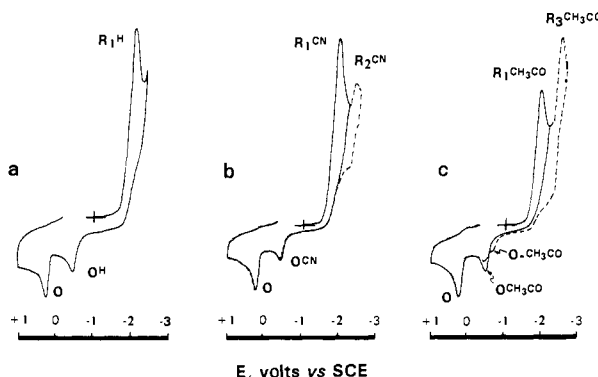


Figure 2. Cyclic voltammograms of $p-ZC_6H_4Pd^{II}Cl(PPh_3)_2$, 2 mM, in THF, with 0.3 M NBu_4BF_4 , at a gold disk electrode (i.d. 0.125 mm). Scan rate $10 V \cdot s^{-1}$. At $20^\circ C$. Z = H (a), CN (b), or CH_3CO (c).

Under these conditions, cyclic voltammetry of $C_6H_5Pd^{II}I(PPh_3)_2$ (compare Figure 1) shows that its reduction wave, R_1^H , is chemically irreversible (up to scan rates of $500 V \cdot s^{-1}$) and corresponds to an overall two-electron process ($n = 1.9 \pm 0.15$).^{12b} Moreover, reduction of $C_6H_5Pd^{II}I(PPh_3)_2$ results also in the formation of " $Pd^0(PPh_3)_2$ ", as evidenced by the appearance of its oxidation wave O on the anodic trace in Figure 1.¹⁵

These series of observations allow delineation of the general mechanistic features of palladium-catalyzed electrocarboxylation of organic halides, which are summarized in Scheme I. All the steps of the catalytic chain are well documented,^{9,11} except its crucial steps, viz., the reduction of the (σ -phenyl)palladium(II) derivative and the reaction(s) of the resulting activated organic moiety leading eventually to the acid and regeneration of the catalyst. In the following we want therefore to focus our attention on these processes. We will first examine them in the absence of a purposely added electrophile and then examine any modification introduced by the presence of an electrophile such as proton or carbon dioxide.

Reduction Mechanism of (σ -Phenyl)palladium(II) Intermediates in the Absence of a Purposely Added Electrophile. Several substituted (σ -aryl)palladium(II) derivatives, $p-ZC_6H_4Pd^{II}X(PPh_3)_2$,

(15) (a) As established by comparison to the oxidation wave of " $Pd^0(PPh_3)_2$ " observed in the reduction of $Pd^{II}X_2(PPh_3)_2$, X = Cl, Br, or I.¹¹ (b) In the following, the electrogenerated zerovalent palladium species is denoted by " $Pd^0(PPh_3)_2$ "; yet we have shown^{11b} that under the experimental conditions used in this study it consists mainly of an anionic species, $Pd^0(PPh_3)_2Cl^-$, resulting from coordination of the low-ligated zerovalent palladium center by a halide ion. (c) Note that the reoxidation wave of " $Pd^0(PPh_3)_2$ " observed in cyclic voltammetry in the absence of added chloride ions appears to be only ca. 60% of what it should be according to a stoichiometric production of the species and its stoichiometric oxidation. As it has been established thoroughly in a previous work,¹¹ this phenomenon is due to the involvement of several equilibria which occur while the anodic sweep of the voltammogram is performed. The reoxidation process occurs then via the partial involvement of CE¹⁸ mechanisms. Under double step chronoamperometric conditions^{18,19} this complication is not observed, as evidence by the value of $[i(2\theta)/i(\theta)] \approx -0.293$.^{11b,18}

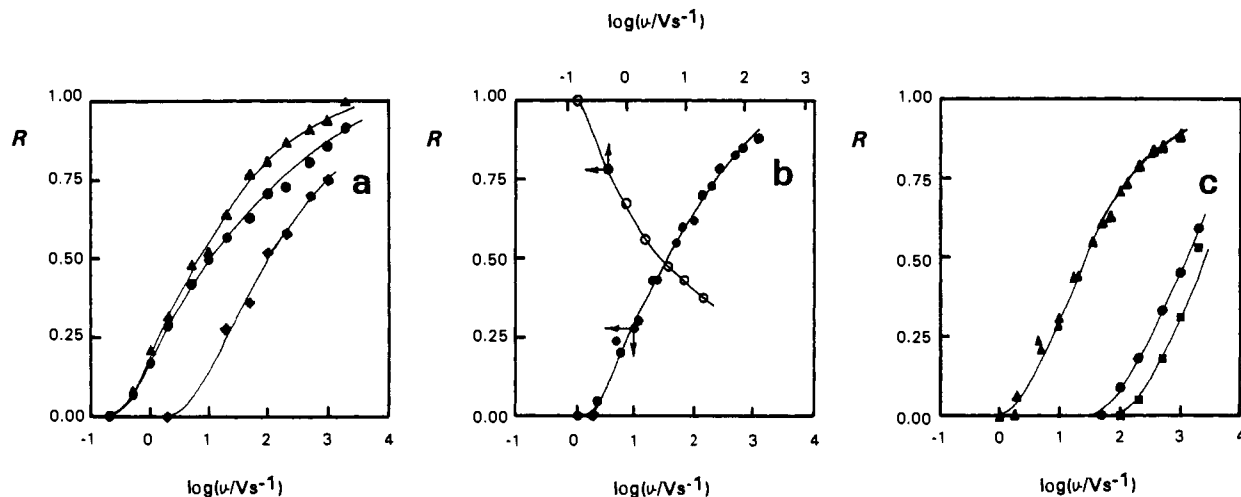
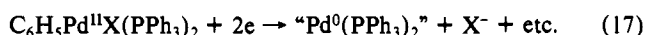


Figure 3. Cyclic voltammetry results for $p\text{-ZC}_6\text{H}_4\text{Pd}^{\text{II}}\text{X}(\text{PPh}_3)_2$, 2 mM, in THF, 0.3 M NBu_4BF_4 , at a gold disk electrode (i.d. 0.125 mm, for $v \geq 10 \text{ V}\cdot\text{s}^{-1}$; i.d. 0.5 mm, for $v < 10 \text{ V}\cdot\text{s}^{-1}$). Variations of the relative peak current intensities of waves O and O^{Z} [$R = i^{\text{p}}_{\text{O}^{\text{Z}}} / (i^{\text{p}}_{\text{O}} + i^{\text{p}}_{\text{O}^{\text{Z}}})$, filled symbols in a, b, c] and of waves R_1^{CN} and R_2^{CN} [$R = 2i^{\text{p}}_{\text{R}_2^{\text{CN}}} / (i^{\text{p}}_{\text{R}_1^{\text{CN}}} + 2i^{\text{p}}_{\text{R}_2^{\text{CN}}})$,²¹ open circles in b]. (a) $Z = \text{H}$, $X = \text{Cl}$ (\blacktriangle), Br (\bullet) and I (\blacklozenge). (b) $Z = \text{CN}$, $X = \text{Br}$. (c) $Z = \text{CN}$, $X = \text{Br}$; (\blacktriangle) alone, (\bullet) in the presence of $\text{C}_6\text{H}_5\text{OH}$, 2 mM, or (\blacksquare) in the presence of CO_2 , 7 mM.

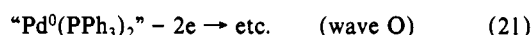
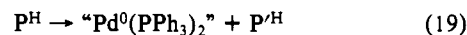
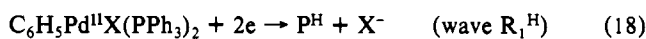
$Z = \text{CN}$ ($X = \text{Br}$), CH_3CO ($X = \text{Br}$), H ($X = \text{Cl}$, Br , I), CH_3 ($X = \text{I}$), have been prepared according to classical procedures¹⁶ by the reaction of the corresponding para-substituted halobenzenes with zerovalent palladium, $\text{Pd}^0(\text{PPh}_3)_4$, and their cyclic voltammetry was examined as a function of scan rate. It is observed, as expected,⁷ that the voltammetric reduction is not influenced significantly by a change of halogen, except for a slight variation of the peak potential of wave R_1^{Z} (compare Table II). The effect of the phenyl substituent results in more drastic changes, as evidenced by the three representative voltammograms shown in Figure 2. When $Z = \text{H}$ (Figure 2a), a single, two-electron irreversible reduction wave, R_1^{H} is observed. It is associated with the formation of two products, whose oxidation waves, O^{H} and O , are detected on the anodic trace.^{17a} It is noteworthy that waves O and O^{H} are independent of the halide, as shown in Table II; this evidences that the halide ion is expelled during the reduction occurring at wave R_1^{H} . Moreover, wave O is identical with that featuring the two-electron oxidation of " $\text{Pd}^0(\text{PPh}_3)_2$ ",^{11,15} suggesting that the latter is produced upon the reduction at wave R_1^{H} , with other products, including that oxidized at wave O^{H} :



The respective magnitude of the peak currents^{17a} of waves O^{H} and O is dependent on scan rate, wave O vanishing at high scan rates, as shown by the variations of $R = i^{\text{p}}_{\text{O}^{\text{H}}} / (i^{\text{p}}_{\text{O}^{\text{H}}} + i^{\text{p}}_{\text{O}})$ in Figure 3a.^{17b} Moreover a double step chronoamperometric investigation^{19a} shows that the sum of the anodic currents of waves O^{H} and O normalized to that of the cathodic current of wave R_1^{H} , viz.,

$[(i_{\text{O}^{\text{H}}} + i_{\text{O}}) / i_{\text{R}_1^{\text{H}}}]_{\theta}$, is constant and close to 0.293^{19b} irrespective of the step time duration θ (0.1–100 ms). This series of results establishes (i) that the product P^{H} , detected by its oxidation wave O^{H} , decays with time to afford " $\text{Pd}^0(\text{PPh}_3)_2$ ", the latter being oxidized at wave O , and (ii) that " $\text{Pd}^0(\text{PPh}_3)_2$ " and P^{H} , whose oxidations require two electrons each, are the only palladium-containing products resulting from the reduction of $\text{C}_6\text{H}_5\text{Pd}^{\text{II}}\text{X}(\text{PPh}_3)_2$ at wave R_1^{H} .^{19b} These conclusions are best summarized by the sequence of reactions in Scheme II:

Scheme II



where P^{H} , a species containing no palladium center, is not detectable by either oxidation or reduction under our conditions (however, vide infra when Z is an electron-withdrawing group).

A very close situation is obtained for $Z = \text{CN}$ (Figure 2b), except that now two reduction waves, R_1^{CN} and R_2^{CN} , are observed, the second one being chemically reversible. Upon scan reversal, they are followed by a set of two oxidation waves,¹⁷ a situation very reminiscent of that observed in Figure 2a. It is noteworthy that the oxidation pattern is almost independent of the fact that the negative scan is extended so as to encompass wave R_2^{CN} or not. Moreover, one of the oxidation waves is identical with wave O , observed for $Z = \text{H}$, whereas the peak potential of the other, O^{CN} , is slightly less negative than that of its homolog O^{H} (compare Table II). The normalized sum of the peak currents of the two oxidation waves is again time independent, and its magnitude establishes that these two waves correspond altogether to a two-electron reoxidation of all palladium-containing species.²⁰ The variations of their relative peak currents are represented in Figure 3b as a function of the scan rate. It is seen that these variations are akin to those observed in Figure 3a for $Z = \text{H}$. They evidence that the product, P^{CN} , oxidized at wave O^{CN} , also decays with time to afford " $\text{Pd}^0(\text{PPh}_3)_2$ ", whose oxidation occurs at wave O .¹¹ Let us now focus our attention on the reduction waves. The first one, R_1^{CN} , is chemically irreversible and involves a two-electron consumption irrespective of the scan rate,^{20,21c} as was observed

(16) (a) Fitton, P.; Johnson, M. P.; Mc Keon, J. E. *J. Chem. Soc., Chem. Commun.* **1968**, 6. (b) Fitton, P.; Rick, E. A. *J. Organomet. Chem.* **1971**, *28*, 287.

(17) (a) The magnitudes of the anodic waves appear to be considerably smaller than those of the reduction waves. This is due to a partial loss of products because of their diffusion away from the electrode while the potential is scanned positively. (b) This ratio incorporates a contribution due to diffusion, owing to the different potential locations of the two waves; thus, the yield in the product oxidized at wave O^{Z} ($Z = \text{H}$, CN , CH_3CO) is smaller than suggested by the magnitude of $R = i^{\text{p}}_{\text{O}^{\text{Z}}} / (i^{\text{p}}_{\text{O}^{\text{Z}}} + i^{\text{p}}_{\text{O}})$. See refs 18 and compare: Kuchynka, D. J.; Amatore, C.; Kochi, J. K. *Inorg. Chem.* **1986**, *25*, 4087. However, these distortions due to diffusion are taken into account in the simulation of voltammograms (compare the working curve in Figure 5).

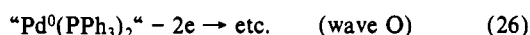
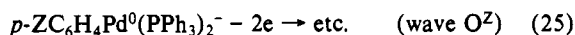
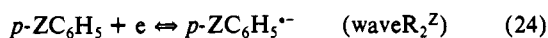
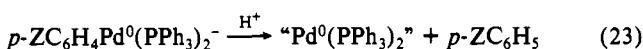
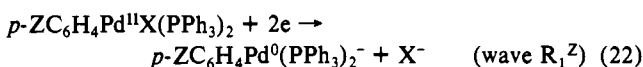
(18) Bard, A. J.; Faulkner, L. R. *Electrochemical Methods*; Wiley: New York, 1980.

(19) (a) The first potential step, of duration θ , was performed on the plateau of wave R_1^{H} and was followed by a second potential step of identical duration on the plateau of wave O . (b) For a chemically reversible system the ratio of the currents at 2θ and θ is $[i(2\theta)/i(\theta)] = 2^{-1/2} - 1 \approx -0.293$.¹⁸ The same result applies for the case of the more complicated kinetic sequences considered here, provided that each oxidation occurring at waves O^{Z} and O involves two electrons (see, e.g., refs 11 and Kuchynka et al. in footnote 17b).

(20) This is established by the comparison of the peak currents to the case $Z = \text{H}$, where this result has been quantitatively established by double step chronoamperometry (vide supra).

for $Z = \text{H}$. Its peak potential is also close to that of wave R_1^{H} , although slightly less negative (compare Table II), in agreement with the electron-withdrawing properties of the cyano substituent. The second reduction wave, R_2^{CN} , is chemically reversible and identical with that observed for an authentic sample of benzonitrile. Its peak current is time dependent, increasing upon decreasing the scan rate. Moreover, its variations as a function of the scan rate parallel those of wave O (compare Figure 3b).²¹ This is evidence that the amount of benzonitrile reduced at wave R_2^{CN} (i) results from further evolution of the product, P^{CN} , formed upon reduction at wave R_1^{CN} and (ii) is formed concomitantly with " $\text{Pd}^0(\text{PPh}_3)_2$ ". This allows one to detail further the mechanism proposed above in Scheme II. On the one hand the product labeled P^{Z} ($Z = \text{H}$ in Scheme II) is now identified as the protonated aryl ligand of the starting material. On the other hand, because of matter conservation, this result imposes that P^{Z} , the primary product of the two-electron reduction at wave R_1^{Z} , must be the anionic zerovalent palladium species: $p\text{-ZC}_6\text{H}_4\text{Pd}^0(\text{PPh}_3)_2^-$.²² These conclusions are summarized in Scheme III.

Scheme III



The mechanism in Scheme III is further supported by the results obtained for the reduction of $p\text{-CH}_3\text{COC}_6\text{H}_4\text{Pd}^{\text{II}}\text{X}(\text{PPh}_3)_2$. At low scan rates (less than $1 \text{ V}\cdot\text{s}^{-1}$) the voltammetry of the acetyl derivative is akin to that observed when $Z = \text{CN}$, in agreement with the comparable electron-withdrawing characters of the cyano and acetyl substituents; thus two reduction waves, $R_1^{\text{CH}_3\text{CO}}$ and $R_2^{\text{CH}_3\text{CO}}$, are followed by the observation of wave O only during the anodic scan. In agreement with the general formulation in Scheme III, wave $R_2^{\text{CH}_3\text{CO}}$ features the reduction of acetophenone, as checked with an authentic sample. The latter is produced almost quantitatively, via eqs 22 and 23, at scan rates less than $1 \text{ V}\cdot\text{s}^{-1}$. Increasing the scan rate results in a decay of wave $R_2^{\text{CH}_3\text{CO}}$ and progressive overlapping of the two reduction waves,^{21c} with the consequence that at scan rates above $10 \text{ V}\cdot\text{s}^{-1}$ one single irreversible wave is observed. In this time domain a second oxidation wave, $O^{\text{CH}_3\text{CO}}$, is also observed within the same potential range where waves O^{H} or O^{CN} are observed (compare Table II and Figure 2c). In agreement with the formulation in Scheme III, the growth of wave $O^{\text{CH}_3\text{CO}}$ upon increasing the scan rate occurs with a concomitant decay of wave O. However, a peculiar

(21) (a) In Figure 3b, the top horizontal scale has been shifted by 0.875 logarithm units with respect to the bottom scale (actual experimental scan rate values) to account for the difference in time delays due to the different potential locations of the waves. Compare ref 7a. Also, due to a difference in diffusion coefficients of benzonitrile and (σ -aryl)palladium species, as well as a difference in electrochemical kinetics, the current peak of the benzonitrile reduction wave has been normalized by considering that the production of benzonitrile was quantitative at scan rates smaller than $0.1 \text{ V}\cdot\text{s}^{-1}$. (b) In $R = 2i_{\text{P}^{\text{R}_2^{\text{CN}}}}/i_{\text{P}^{\text{R}_1^{\text{CN}}}} + 2i_{\text{P}^{\text{R}_2^{\text{CN}}}}/i_{\text{P}^{\text{R}_1^{\text{CN}}}}$, the double of the benzonitrile normalized peak current is used to account for the fact that benzonitrile gives a one-electron wave, while the arylpalladium(II) complex is reduced along a two-electron wave.^{12b} A proper interpretation of R variations would require a perfect knowledge of the electrochemical reduction mechanisms occurring at waves R_1^{Z} , O, and O^{Z} . (c) Any attempt to characterize these processes kinetically failed since all these waves are controlled by overall kinetics of charge transfer with half-widths about 130–150 mV and shifts of their peak potentials by ca. 90–100 mV/unit of $\log v$. Although this suggests¹⁸ α values on the order of 0.3 (upon considering that the kinetics is controlled by the first electron exchange), no detailed chemical meaning can be inferred from such values, since it is not known whether the initial electron transfer is concerted or not with bond breaking (R_1^{Z}) or bond formation (O and O^{Z}).

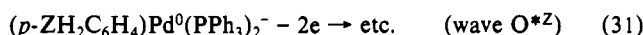
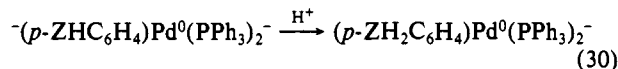
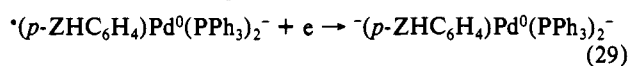
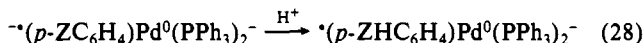
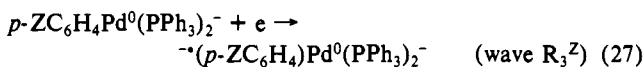
(22) (a) Owing to matter conservation, the product oxidized at wave O^{Z} must contain (i) a $\text{Pd}^0(\text{PPh}_3)_2$ moiety and (ii) an aryl ligand. (iii) In addition, we know that it does not contain halide ion (vide supra and Table II). $p\text{-ZC}_6\text{H}_4\text{Pd}^0(\text{PPh}_3)_2^-$ is the minimal chemical structure that meets all the above requirements. (b) Compare to $\text{ClPd}^0(\text{PPh}_3)_2^-$ or $\text{BrPd}^0(\text{PPh}_3)_2^-$ in ref 11b.

Table III. Cyclic Voltammetry of $p\text{-CNC}_6\text{H}_4\text{Pd}^{\text{II}}\text{Br}(\text{PPh}_3)_2$, 2 mM, at a Gold Disk Electrode (i.d. 0.125 mm), at 20°C . Peak Potentials ($100 \text{ V}\cdot\text{s}^{-1}$) of Waves R_1^{CN} , R_2^{CN} , O^{CN} , and O relative to That of the Benzonitrile Reduction Wave, as a Function of Solvent^{a,b}

solvent	$\Delta E_{\text{P}^{\text{R}_1^{\text{CN}}}}^{\text{P}^{\text{R}_1^{\text{CN}}}}$	$\Delta E_{\text{P}^{\text{R}_2^{\text{CN}}}}^{\text{P}^{\text{R}_2^{\text{CN}}}}$	$\Delta E_{\text{O}^{\text{CN}}}^{\text{O}^{\text{CN}}}$	$\Delta E_{\text{O}}^{\text{O}}$	$v_{1/2} (\text{V}\cdot\text{s}^{-1})^c$
THF	0.37	0.00	1.95	2.60	28
DMF	0.29	0.00	1.85	2.43	200
DMSO	0.17	0.00	1.85	2.39	750

^a Containing 0.3 M NBu_4BF_4 . ^b $\Delta E_{\text{P}^{\text{X}}}^{\text{P}^{\text{X}}} = E_{\text{P}^{\text{X}}}^{\text{P}^{\text{X}}} - E_{\text{P}^{\text{benzonitrile}}}^{\text{P}^{\text{benzonitrile}}}$. ^c Scan rate required for the peak currents of waves O^{CN} and O to be identical (see text).

additional feature is observed for this system, due to the intrinsic reducibility of the acetophenone moiety.²³ Thus, when the negative scan is extended to ca. -2.8 V , a third, two-electron irreversible reduction wave, $R_3^{\text{CH}_3\text{CO}}$, is observed, as shown in Figure 2c. For scan rates around $10 \text{ V}\cdot\text{s}^{-1}$, scanning over this wave results in the appearance of a third oxidation wave, $O^{\text{CH}_3\text{CO}}$, observed at a more negative potential than wave $O^{\text{CH}_3\text{CO}}$. Simultaneously, the peak current of wave $O^{\text{CH}_3\text{CO}}$ decays. At higher scan rates ($100 \text{ V}\cdot\text{s}^{-1}$ or above) wave $R_3^{\text{CH}_3\text{CO}}$ becomes reversible and involves the consumption of one electron. Under these circumstances, wave $O^{\text{CH}_3\text{CO}}$ disappears, wave $O^{\text{CH}_3\text{CO}}$ being restored at its full magnitude (i.e., its peak current is almost independent of whether the potential scan is extended to encompass wave $R_3^{\text{CH}_3\text{CO}}$ or not). A qualitative explanation for this peculiar behavior consists in considering that the kinetic sequence in Scheme III may be complicated by the reduction, at wave $R_3^{\text{CH}_3\text{CO}}$, of the p -acetylphenyl ligand of the anionic palladium species formed at wave $R_1^{\text{CH}_3\text{CO}}$ (eq 22). At moderate scan rates, this would lead, via an ECE/DISP²⁴ classical sequence, to the two-electron, two-proton reduction of the carbonyl bond into the corresponding alcohol:²³



where ZH_2 represents a $\text{CH}_2\text{CH}(\text{OH})$ substituent. The relative positions of waves $O^{\text{CH}_3\text{CO}}$ and $O^{\text{CH}_3\text{CO}}$ (see Table II) are in qualitative agreement with the respective electronic effects of a Z (i.e., CH_3CO) or a ZH_2 substituent. Therefore, besides introducing more complexity in the interpretation of the voltammetry of the acetyl derivative, this peculiar behavior is an additional indirect proof of the validity of the attribution of wave O^{Z} to the oxidation of a phenyl-containing (and palladium-containing) species. However, for most of the following studies the cyano derivative was chosen as a model compound, since its cyclic voltammetry represents all the significant mechanistic features outlined in Scheme III, without the additional peculiar behaviors observed for the cases where $Z = \text{H}$ or CH_3 (viz., the nonobservation of wave R_2^{Z} because of the nonreducibility of benzene) or $Z = \text{CH}_3\text{CO}$ (viz., the progressive overlapping of waves R_1^{Z} and R_2^{Z} and further mechanistic complication due to the carbonyl reduction in the sequence of eqs 27–31).

Effect of Changing the Solvent. On qualitative grounds, the voltammetry of the (σ - p -cyanophenyl)palladium(II) derivative remains identical when THF is changed to more polar and less

(23) For a review on reduction of carbonyls into the corresponding alcohols, see, e.g.: Baizer, M. M. In *Organic Electrochemistry*; Lund, H., Baizer, M. M., Eds.; Marcel Dekker: New York, 1991; pp 433f.

(24) (a) Amatore, C.; Gareil, M.; Savéant, J. M. *J. Electroanal. Chem. Interfacial Electrochem.* 1983, 147, 1. (b) Amatore, C. In *Organic Electrochemistry*; Lund, H., Baizer, M. M., Eds.; Marcel Dekker: New York, 1991; pp 76, 77.

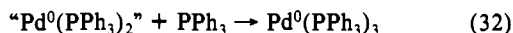
Table IV. Cyclic Voltammetry Data for *p*-ZC₆H₄Pd^{II}X(PPh₃)₂, 2 mM, in THF, with 0.3 M NBu₄BF₄, as a Function of Additive. Values of Scan Rates, *v*_{1/2}, Required for the Peak Currents of Waves O^Z and O to be Identical. Gold Disk Electrode (i.d. 0.125 mm), at 20 °C

<i>p</i> -ZC ₆ H ₄ Pd ^{II} -X(PPh ₃) ₂		additive (concn)	<i>v</i> _{1/2} (V·s ⁻¹)
Z	X		
CH ₃	I	none	65
H	Cl	none	100
H	Br	none	8.0
H	I	none	5.3 ^a
		PPh ₃ (5 mM)	150 ^a
		PPh ₃ (10 mM)	280 ^a
		PPh ₃ (20 mM)	550 ^a
CH ₃ CO	Br	none	10
CN	Br	none	28 ^b
		PPh ₃ (5 mM)	400 ^b
		PPh ₃ (10 mM)	900 ^b
		PPh ₃ (20 mM)	1600 ^b
		C ₆ H ₅ OH (2 mM)	1100
		C ₆ H ₅ OH (2 mM) + PPh ₃ (5 mM)	3000
		CO ₂ (5 mM)	1900
		CO ₂ (5 mM) + PPh ₃ (2.5 mM)	3200

^a *v*_{1/2} (V·s⁻¹) = 9.2 + 27.1 [PPh₃] (mM); correlation coefficient 0.999. ^b *v*_{1/2} (V·s⁻¹) = 36.8 + 79.5 [PPh₃] (mM); correlation coefficient 0.998.

aprotic solvents such as DMF^{3h,14b} or DMSO. Table III presents the variations of the peak potential of the four waves involved in the corresponding voltammograms. Table III also gives the value, *v*_{1/2}, of the scan rate required for the peak currents of waves O and O^{CN} to be identical, this measure being almost directly related to the inverse of the lifetime, *t*_{1/2}, of the anionic species *p*-CNC₆H₄Pd⁰(PPh₃)₂⁻.²⁵ Comparison of the data in the last column of Table III shows that the rate of dissociation of this intermediate increases drastically with the proton-donor and coordinating abilities of the solvent. Such a result is in qualitative agreement with a thermodynamically favored dissociation upon increasing the solvent ability to solvate/protonate the aryl anion and to coordinate the low-ligated zerovalent palladium species, "Pd⁰(PPh₃)₂". To examine the validity and possible generality of this latter point, we examined the kinetic effects due to an addition of PPh₃ or of halide ions to the medium. Indeed, these species are expected to stabilize the zerovalent palladium moiety.^{11b}

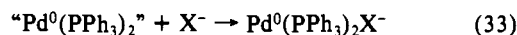
Effect of Addition of PPh₃. Addition of PPh₃, 5–20 mM, to the system in THF does not result in a qualitative change of the voltammetry of the (*σ*-*p*-cyanophenyl)palladium(II) derivative, except for a drastic increase of the rate of dissociation of the intermediate oxidized at wave O^{CN} and an expected change in the shape of wave O due to the easy coordination of "Pd⁰(PPh₃)₂" by triphenylphosphine:^{11b}



A similar effect was observed for the unsubstituted phenyl derivative (Z = H). Both series of results are summarized in Table IV, under the form of the variations of *v*_{1/2}, the scan rate such that the peak currents of waves O and O^Z are equal (vide supra),²⁵ as a function of the phosphine concentration. It is noteworthy that a good linear correlation is observed between *v*_{1/2} (in V·s⁻¹) and [PPh₃] (in mM): *v*_{1/2} = 9.2(1 + 2.9[PPh₃]), for Z = H and X = I (entries 4–7 of Table IV; correlation coefficient 0.999), and *v*_{1/2} = 36.8(1 + 2.2[PPh₃]), for Z = CN and X = Br (entries 9–12 of Table IV; correlation coefficient = 0.998).

Effect of Halide Ions. As noted above (compare Table II), the peak potential of wave O^Z observed in the voltammetry of *p*-ZC₆H₄Pd^{II}X(PPh₃)₂ was insensitive to the nature of the halide ion present in the (*σ*-aryl)palladium(II) derivative, depending only on the nature of the substituent Z. In apparent contrast with this

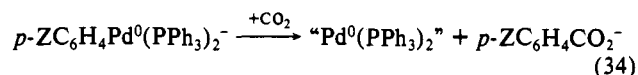
result, the rate of disappearance (eq 23) of the species oxidized at wave O^Z was influenced by the nature of the halide as is evident, e.g., in Figure 3a for Z = H. Table IV shows that this rate increased by a factor of 20 when going from iodine (fourth entry of Table IV) to chlorine (second entry of Table IV). A similar effect is noticed when the voltammetries are performed in the presence of purposely added halide ions. For example, the addition of a 5-fold excess of *n*-Bu₄NBr to a solution of *p*-CNC₆H₄Pd^{II}Br(PPh₃)₂, 2 mM, resulted in an increase of *v*_{1/2} by a factor of 2 and in a modification of the shape and peak potential of wave O. On the basis of our previous studies,^{11b} these effects can be easily rationalized by considering that the low-ligated zerovalent species, "Pd⁰(PPh₃)₂", produced in eq 23 is stabilized by halide ions (Cl⁻ >> Br⁻ > I⁻):



On kinetic grounds, the situation is then equivalent to, although less effective than, that observed in the presence of added phosphine.

Effect of an Added Electrophile. The formulation given in Scheme III to describe the formation of "Pd⁰(PPh₃)₂" from the anionic (*σ*-aryl)palladium(0) complex requires a proton source. In the THF solutions investigated this proton source may consist of residual water or the tetrabutylammonium cation.^{14b} To avoid possible complications due to such weak or difficultly controllable proton sources, phenol was added to the medium so as to investigate the role of a proton donor. Thus addition of a 1 equiv of phenol resulted in an increase of the rate of the overall reaction in eq 23 by a factor ca. 40, as shown by the corresponding increase of *v*_{1/2},²⁵ the scan rate required for the peak currents of waves O and O^Z to be equal (compare Table IV, entries 9 and 13, and Figure 3c for Z = CN). In agreement with the formulation in Scheme III, the decay of wave O^Z in the presence of phenol was associated with a concomitant increase of the aromatic reduction wave, as could be observed for Z = CN.

Similar effects were observed when carbon dioxide was added to the medium instead of phenol. At any given scan rate, wave O grew at the expense of wave O^Z, thus requiring a larger *v*_{1/2} value so that *i*_{P^{OZ}} = *i*_{P^O} (see, e.g., Figure 3c for Z = CN). As shown in Table IV, entries 9 and 15, the addition of CO₂, 5 mM, resulted in an increase of the rate of disappearance of wave O^{CN} by a factor ca. 65. Moreover, in the presence of carbon dioxide, the fading-out of waves O^Z was not associated with a production of the aromatic compound, since even at small scan rates its reduction wave remained vanishingly small, as could be established when Z = CN. Such a finding is in agreement with the preparative scale results, since, in the presence of CO₂, the main reaction product is the arenecarboxylate (compare Table I and ref 3h). This establishes that the overall reaction of the anionic species formed in eq 22 (Scheme III) with carbon dioxide is faster than its reaction with the medium in eq 23:



Effect of the Palladium Complex Concentration. Figure 4 presents a series of voltammograms for the (*p*-cyanophenyl)-palladium(II) *σ*-complex, as a function of its concentration. To avoid possible kinetic complications, these experiments were performed in the presence of excesses of halide ions, triphenylphosphine, and phenol. Comparison of the respective sizes of waves R₂^{CN}, O^{CN}, and O clearly demonstrates that the palladium complex concentration drastically affects the overall kinetics. Increasing its concentration results in a decrease of the rate of the overall reaction in eq 23 of Scheme III, as evidenced by the decrease of wave R₂^{CN} and the increase of wave O^{CN}. Such a behavior clearly establishes that eq 23 (or eq 34) cannot be an elementary step as suggested by its above formulation, but necessarily involves a complex sequence of reactions.

Discussion

All the previous results are in qualitative agreement with the general formulation in Scheme III, establishing that electron-

(25) At a given scan rate, *v*, the time elapsed between scanning wave R₂^Z and wave O^Z is *t* ≈ (E_{P^{R₂^Z} + E_{P^{OZ}} - 2E_{inv})/*v*, where *v* is the scan rate, E_{inv} is the potential of scan inversion, and the E_P's are the respective potential peaks of the two waves (compare ref 11b). Thus *t*_{1/2} ≈ (E_{P^{R₂^Z} + E_{P^{OZ}} - 2E_{inv})/*v*_{1/2}.}}

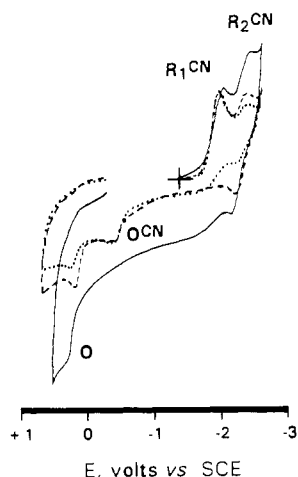
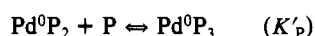
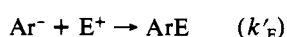
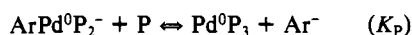


Figure 4. Cyclic voltammogram of $p\text{-CNC}_6\text{H}_4\text{Pd}^{\text{II}}\text{X}(\text{PPh}_3)_2$ in THF, with 0.3 M NBu_4BF_4 , at a gold disk electrode (i.d. 0.125 mm) as a function of the substrate concentration, in the presence of added PPh_3 , 5 mM; $\text{C}_6\text{H}_5\text{OH}$, 5 mM; and NBu_4Br , 5 mM. Scan rate $100 \text{ V}\cdot\text{s}^{-1}$. At 20°C . $[p\text{-CNC}_6\text{H}_4\text{Pd}^{\text{II}}\text{X}(\text{PPh}_3)_2] = 1 \text{ mM}$ (solid line), 2 mM (dashed line), or 4 mM (dotted line). Note that the current scales have been adjusted so that the peak current of wave R_1^{CN} is approximately constant, to ease the comparison of the variations of the other waves.

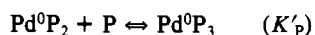
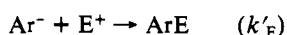
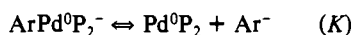
transfer activation of the (σ -aryl)palladium(II) intermediate in Scheme I occurs via an overall two-electron process leading to the formation of an anionic (σ -aryl)palladium(0) derivative. The presence of an added electrophile (proton or carbon dioxide) or of triphenylphosphine did not alter this overall reaction course, as evidenced by the independence of the general voltammetric behavior with respect to these factors, yet they affect drastically the lifetime of the (σ -aryl)palladium(0) anionic intermediate. Therefore, the main mechanistic feature that is not determined at this stage^{21c} deals with the exact nature of the reactions of this intermediate with electrophiles and/or free phosphine. Of importance for the following discussion are the two following facts: (i) the effects of electrophiles and free phosphine have been observed to be cumulative, and (ii) the overall rates of the processes in eqs 23 or 34 are decreased upon increasing the (σ -aryl)palladium(II) complex concentration. Several mechanisms can be conceived that qualitatively agree with these experimental observations. However, most of these kinetic possibilities must be ruled out on the basis of known chemistry. Thus mechanisms that would require an electrophilic attack on the anionic zerovalent palladium to be reversible²⁶ must be eliminated because the reverse reaction would involve the oxidative addition of a zerovalent palladium complex to a carbon-hydrogen (eq 23) or a carbon-carbon bond (eq 34). We have therefore to consider only the two limiting cases summarized in Scheme IV. They have been tentatively classified according to the "associative" or "dissociative" nature of the reactions of $\text{ArPd}^0\text{P}_2^-$ with an electrophile (E^+) or a phosphine ligand (P).

Scheme IV

associative mechanism:



dissociative mechanism:



(26) So as to account for the cumulative effects of added electrophile and phosphine ligand.

Each of these mechanisms corresponds to a particular rate law for the disappearance of the anionic intermediate $\text{ArPd}^0\text{P}_2^-$, i.e., to particular variations of $[\text{P}^0_{\text{Oz}}/(\text{P}^0_{\text{Oz}} + \text{P}^0_{\text{O}})]$ with the scan rate (compare Figure 3). These individual rate laws are given in eqs 35 and 36, respectively, for the associative and the dissociative mechanism ($[\text{Pd}]^b$ represents the initial palladium(II) complex concentration).

$$\frac{d[\text{ArPd}^0\text{P}_2^-]}{dt} = -\{k_E + k'_E K_p [\text{P}] / ([\text{Pd}]^b - [\text{ArPd}^0\text{P}_2^-])\} [\text{E}^+] [\text{ArPd}^0\text{P}_2^-] \quad (35)$$

$$\frac{d[\text{ArPd}^0\text{P}_2^-]}{dt} = -k'_E K K'_p [\text{P}] [\text{E}^+] [\text{ArPd}^0\text{P}_2^-] / ([\text{Pd}]^b - [\text{ArPd}^0\text{P}_2^-]) \quad (36)$$

It is noteworthy that, because of involvement of palladium concentration in their denominators, each rate law predicts a decrease of the overall rate of dissociation of $\text{ArPd}^0\text{P}_2^-$ upon increasing the complex concentration, in agreement with the experimental observations (compare Figure 4). If k_E is not null, the rate law in eq 35 is not symmetrical in $[\text{E}^+]$ and $[\text{P}]$. It therefore suggests a different kinetic behavior with each of these parameters, in contradiction with the experimental observations. We can then conclude that if the associative mechanism is considered, only the limit with $k_E = 0$ has an experimental significance under our conditions. Both mechanisms in Scheme IV correspond then to the same rate law given in eq 37 (where $k^{\text{ap}} = k'_E K_p$ ($[\text{P}][\text{E}^+]$), for the associative mechanism, or $k^{\text{ap}} = k'_E K K'_p$ ($[\text{P}][\text{E}^+]$), for the dissociative one).²⁷ Because of their identical

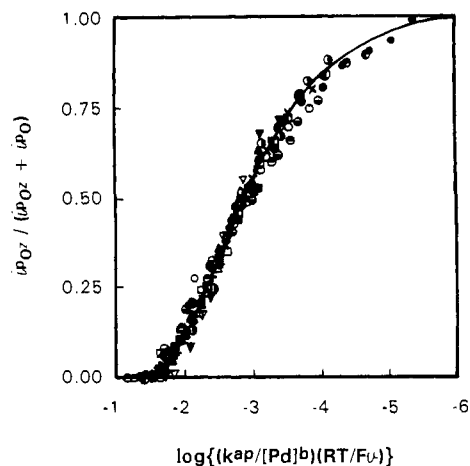
$$\frac{d[\text{ArPd}^0\text{P}_2^-]}{dt} = -(k^{\text{ap}} / [\text{Pd}]^b) [\text{ArPd}^0\text{P}_2^-] / \{1 - ([\text{ArPd}^0\text{P}_2^-] / [\text{Pd}]^b)\} \quad (37)$$

rate laws, the two mechanisms cannot be distinguished on the basis of kinetics. Their only difference is the one-step or two-step nature of the overall substitution, at the zerovalent palladium center, of the aryl ligand, Ar^- , by the phosphine, P. Since this substitution reaction is reversible under our conditions, the mechanistic implications of its exact nature (viz., associative or dissociative) are negligible for our purpose here. For what concerns the reactivity of the aromatic moiety with electrophiles, the two mechanisms can then be considered as minor variants, since both involve a reaction of the electrophile with a free σ -aryl anion, by opposition to a reaction occurring within the palladium coordination shell.

Let us now examine the experimental validity of both mechanisms on quantitative kinetic grounds. Figure 5 shows that the theoretical predictions²⁸ based on the rate law in eq 37 agree satisfactorily with the experimental variations of $[\text{P}^0_{\text{Oz}}/(\text{P}^0_{\text{Oz}} + \text{P}^0_{\text{O}})]$ for all the systems investigated in this study. The resulting values of the overall rate constants k^{ap} (in eq 37, viz., $k'_E K K'_p [\text{P}][\text{E}^+]$ or $k'_E K_p [\text{P}][\text{E}^+]$) are reported in the caption of Figure 5. Owing to the intricate nature of these overall rate constants, any rationalization of their variations as a function of the electronic properties of the phenyl substituent is difficult. On the one hand, it is expected that an electron-withdrawing group will increase the value of the equilibrium constant K_p or ($K K'_p$) because of a larger stabilization of the σ -aryl anion than of the anionic zerovalent center. On the other hand, the stabilization of the σ -aryl anion should result in a decreased rate constant, k'_E , for its reaction with an electrophile.

(27) The concentrations of the electrophile and of the phosphine are included in the expressions of k^{ap} to account for the cases where, in the absence of these reagents, their roles are performed by the medium (vide infra and eqs 40-44).

(28) (a) The working curve in Figure 5 has been simulated considering an average relative position of the three electrochemical waves R_1^Z , O^Z , and O , since the relative variations of $(E^{\text{P}}_{\text{R},z} + E^{\text{P}}_{\text{Oz}} - 2E_{\text{im}})^{25}$ and $(E^{\text{P}}_{\text{O}} - E^{\text{P}}_{\text{Oz}})$ are small (<10%) for the series of systems considered in Figure 5 (compare Table II). Note, however, that on a strict basis each system should be represented on a single working curve derived for the precise relative positions of the three waves. Yet the error introduced by considering a single curve is negligible vis-à-vis that due to the precision of the measurements of P^0_{Oz} and P^0_{O} . (b) For the simulations, the processes at waves R_1^Z , O^Z , and O have been considered as being controlled by the kinetics of electron transfer with α values of 0.3, so as to match the experimental observations.^{21c} (c) Simulations were performed according to a classical explicit finite difference procedure.¹⁸



Symbol	<i>p</i> -Z-C ₆ H ₄ -Pd ^{II} X(PPh ₃) ₂		Medium/ NBu ₄ BF ₄ 0.3 M	Additive	100· <i>k</i> ^{ap} (M·s ⁻¹)
	Z	X			
●	CH ₃	I	THF	none	0.60
○	H	Cl	THF	none	0.93
×	H	Br	THF	none	0.075
●	H	I	THF	none	0.050
■			THF	PPh ₃ , 5 mM	1.4
■			THF	PPh ₃ , 10 mM	2.6
◆			THF	PPh ₃ , 20 mM	5.1
●	CH ₃ CO	Br	THF	none	0.093
○	CN	Br	THF	none	0.26
○			DMF	none	1.9
□			DMSO	none	7.0
▼			THF	PPh ₃ , 5 mM	3.7
▲			THF	PPh ₃ , 10 mM	8.4
▽			THF	PPh ₃ , 20 mM	15
■			THF	C ₆ H ₅ OH, 2 mM	10
*			THF	PPh ₃ , 5 mM + C ₆ H ₅ OH, 2 mM	28
Δ			THF	CO ₂ , 5 mM	18
+			THF	PPh ₃ , 2.5 mM + CO ₂ , 5 mM	30

Figure 5. Cyclic voltammery data for *p*-Z-C₆H₄Pd^{II}X(PPh₃)₂ (1 mM ≤ [Pd]^b ≤ 4 mM), at gold disk electrodes (i.d. 0.125 mm, for *v* ≥ 10 V·s⁻¹; i.d. 0.5 mm, for *v* < 10 V·s⁻¹). At 20 °C. Unifying representation of the variations of the relative peak current intensities of waves O and O² with the scan rate and palladium concentration [compare *R* = *i*_{O²}/(*i*_O + *i*_{O²}) in Figure 3], for the systems investigated in this study. The solid line corresponds to the rate law in eq 37²⁸ with the given values of *k*^{ap}.²⁷

In Figure 5, *k*^{ap} was determined for each situation on the basis of the formulation in eq 37.²⁷ However, a closer inspection of the *k*^{ap} variations as a function of added phosphine concentration shows that *k*^{ap} is not proportional to the latter as predicted from its definition in eq 37 (viz., *k*^{ap} = *k*'_E*K*_P[PPh₃][E⁺], for the associative mechanism, or *k*^{ap} = *k*'_E*K**K*'_P[PPh₃][E⁺]), but rather follows a linear correlation with this parameter, in agreement with the observed correlations of *v*_{1/2} with [PPh₃] (compare Table IV). Thus, for Z = H and X = I (correlation coefficient 0.999),

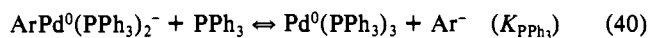
$$k^{ap} = (9.0 \times 10^{-4})(1 + 2.8[\text{PPh}_3]) \quad (38)$$

and for Z = CN and X = Br (correlation coefficient 0.998),

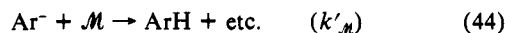
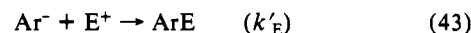
$$k^{ap} = (3.2 \times 10^{-3})(1 + 2.3[\text{PPh}_3]) \quad (39)$$

where *k*^{ap} is in M·s⁻¹ and [PPh₃] in mM. However, such results are not contradictory with the mechanisms in Scheme IV. Indeed, for the sake of simplicity, coordination of "Pd⁰P₂" by a phosphine ligand only was considered in Scheme IV. Yet, at least two other possible ligands exist: the solvent (S) and the halide ion (X⁻).^{11b,29} Therefore, at least three simultaneous (true or overall) equilibria

contribute to the formation of Ar⁻:



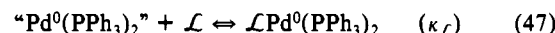
Similarly several electrophiles may compete for reacting with Ar⁻: the medium (M) itself, most presumably involving a protonation by the tetrabutylammonium cation or residual water, and the purposely added electrophile (E⁺).



Consideration of these additional reactions leads to a rate law identical with that in eq 37, yet *k*^{ap} is now expressed as

$$k^{ap} = (k^{ap})_0(1 + \mathcal{H}_{\text{PPh}_3}[\text{PPh}_3])(1 + k_{\text{E}}[\text{E}^+]) \quad (45)$$

where $\mathcal{H}_{\text{PPh}_3} = K_{\text{PPh}_3}/(K_{\text{S}}[\text{S}] + K_{\text{X}}[\text{X}^-])$ and $k_{\text{E}} = k'_{\text{E}}/k'_{\text{M}}[\text{M}]$; $(k^{ap})_0 = k'_{\text{M}}[\text{M}](K_{\text{S}}[\text{S}] + K_{\text{X}}[\text{X}^-])$ is an intrinsic overall rate constant for the particular system and medium considered, viz., the rate constant observed in the absence of added ligand or electrophile. Comparison to the results in eqs 38 and 39 (where [E⁺] = 0) shows that the predictions of eqs 37 and 45 are in agreement with the experimental observations. Moreover, the values of $\mathcal{H}_{\text{PPh}_3}$ (viz., 2.8 mM⁻¹ in eq 38 for Z = H and X = I, and 2.3 mM⁻¹ in eq 39 for Z = CN and X = Br) are reasonably close, as expected. Indeed, each overall equilibrium in eqs 40–42 results in the combination, true or thermochemical, of two reactions, the first one (eq 46) being independent of the ligand L (where L is S, X⁻, or PPh₃ accordingly):



Then, $K_{\text{L}} = K_{\text{Ar}}K_{\text{L}}$, showing that $\mathcal{H}_{\text{PPh}_3} = K_{\text{Ar}}K_{\text{PPh}_3}/(K_{\text{Ar}}K_{\text{S}}[\text{S}] + K_{\text{Ar}}K_{\text{X}}[\text{X}^-]) = K_{\text{PPh}_3}/(K_{\text{S}}[\text{S}] + K_{\text{X}}[\text{X}^-])$, is independent of the aryl ligand. Indeed, $\mathcal{H}_{\text{PPh}_3}$ involves only equilibrium constants that are related to the stabilization of the low-ligated zerovalent palladium, "Pd⁰(PPh₃)₂", in eq 47. Furthermore, from the definition of $(k^{ap})_0$ in eq 45 and using the above relationships, one has the following:

$$\rho = (\mathcal{H}_{\text{PPh}_3})_{\text{H,I}}/(\mathcal{H}_{\text{PPh}_3})_{\text{CN,Br}} = (k_{\text{S}}[\text{S}] + k_{\text{X}}[\text{X}^-])_{\text{Br}}/(k_{\text{S}}[\text{S}] + k_{\text{X}}[\text{X}^-])_{\text{I}} = [(k^{ap})_0]_{\text{H,Br}}/[(k^{ap})_0]_{\text{H,I}} \approx (v_{1/2})_{\text{H,Br}}/(v_{1/2})_{\text{H,I}} \quad (48)$$

where the last term in eq 48 is of the order of 1.5 (as deduced from the third and fourth entries of Table IV). This result is in reasonable agreement with the value of ρ (viz., 2.8/2.3 = 1.2) deduced from the slopes of the correlations in eqs 38 and 39.

Let us consider now the reaction of Ar⁻ with electrophiles. The formulation in eq 45 predicts that the ratio of the overall rate constants *k*^{ap}, in the presence or in the absence of electrophile, represents directly the value of (1 + *k*_E[E⁺]). Thus, from the data in Figure 5 and in Table IV (9th and 13th entries for phenol, 9th and 15th for carbon dioxide), one shows that Ar⁻ (Z = CN) reacts ca. 40 times faster with C₆H₅OH, 2 mM, and ca. 70 times faster with CO₂, 5 mM, than it is protonated by the medium in the absence of added electrophile or proton donor. This drastic increase of rate in the presence of CO₂ explains why, under preparative scale conditions, the arenecarboxylate is the major reaction product in the presence of carbon dioxide (note that [CO₂] ≈ 0.2 M¹³ under the conditions of Table I). Yet, in apparent contradiction with the formulation in eq 45, these numbers are significantly reduced in the presence of added phosphine. Thus, the reaction with phenol (2 mM) is only ca. 7.5 times faster than the reaction with the medium when 5 mM PPh₃ is present in the medium. Similarly, the reaction with CO₂ (5 mM) is only ca. 13.5 times faster than that with the medium when 2.5 mM PPh₃ is present in the medium. This suggests that in the absence of a purposely added ligand, such as PPh₃, the phenolate or car-

(29) Negishi, E. I.; Takahashi, T.; Akiyoshi, K. *J. Chem. Soc., Chem. Commun.* 1986, 1338.

tion was used.³⁷ The reference electrode was an SCE (Tacussel) separated from the solution by a bridge (3 mL) filled with a *n*-Bu₄NBF₄ solution in THF identical with that used in the cell. All potentials given here refer to this reference electrode. All the experiments reported here were performed at 20 °C.

Electron consumptions in transient electrochemistry were determined following a method previously described that combines the use of classical working electrodes and ultramicroelectrodes.⁹ Other electrochemical procedures are identical with those previously described.¹¹ Carbon dioxide concentration was determined according to the procedure described in ref 3p.

Preparative Scale Reductions of (σ -Aryl)palladium(II) Complexes in the Presence of Carbon Dioxide. The divided cell, experimental setup, and procedures were identical with those previously described.^{3p,11} Anhydrous carbon dioxide (Air Liquide) was continuously bubbled through the solution during the electrolysis so as to ensure constantly a saturating concentration. Electrolyses were performed with 0.5 mmol of starting material dissolved in 50 mL of THF, 0.3 M NBu₄BF₄ (catholyte). A lithium rod was used as a sacrificial anode (anolyte: 15–20 mL of THF, 0.3 M NBu₄BF₄). The electrolyses were interrupted when the current reached 5–6 mA (limit for background current). The catholyte was poured into 200 mL of sodium hydroxide solution (1 N in water). The mixture was extracted three times with 80 mL of Et₂O. The organic phase was dried over MgSO₄, filtered, and evaporated. Aromatic compounds were identified (Ar–Ar; no ArH derivative could be observed) and titrated using 250-MHz ¹H NMR, by dissolving the residue in 1 mL of

(37) Amatore, C.; Lefrou, C.; Pflüger, F. J. *Electroanal. Chem. Interfacial Electrochem.* 1989, 270, 43.

CDCl₃ with 1,1,2,2-tetrachloroethane as an internal standard, and comparison with authentic samples. The aqueous phase was acidified to pH = 3–4 with HCl, 1 N. It was then extracted three times with 80 mL of Et₂O, dried over MgSO₄, filtered, and evaporated. The yield in ArCO₂H was then determined using 250-MHz ¹H NMR, by dissolving the residue in 1 mL of CDCl₃ with 1,1,2,2-tetrachloroethane as an internal standard, and comparison with authentic samples of the carboxylic acids. For the case of the cyano derivative, *p*-terephthalic acid was isolated, owing to the facile hydrolysis of the cyano group under the basic conditions prevailing either during the electrolysis or during the workup of the solution.

Acknowledgment. This work has been supported in part by CNRS (URA 1110 Activation Moléculaire) and by ENS. Partial financial support from SNPE (Contract No. 14/89) and EDF (Contract No. OT-E53L31) is also acknowledged. Mr. Serge Negri is acknowledged for his kind technical assistance during some of the electrochemical experiments reported in Table I.

Registry No. Pd^{II}Cl₂(PPh₃)₂, 13965-03-2; Pd^{II}Cl₂(PBu₃)₂, 14977-08-3; Pd^{II}Cl₂(dppe), 19978-61-1; Pd^{II}Cl₂(dpp), 59831-02-6; C₆H₅Pd^{II}Br(dppe), 142438-84-4; C₆H₅Pd^{II}Br(PPh₃)₂, 30643-33-5; C₆H₅Pd^{II}Br(PPh₃)₂, 30643-33-5; *p*-CH₃C₆H₄Pd^{II}I(PPh₃)₂, 142507-62-8; *p*-CH₃COC₆H₄Pd^{II}Br(PPh₃)₂, 37474-29-6; *p*-CNC₆H₄Pd^{II}Br(PPh₃)₂, 142507-61-7; Pd⁰(PPh₃)₄, 14221-01-3; C₆H₅Pd^{II}Cl(PPh₃)₂, 63864-53-9; C₆H₅Pd^{II}I(PPh₃)₂, 55123-60-9; PPh₃, 603-35-0; *p*-CNC₆H₄Br, 623-00-7; C₆H₅CO₂H, 65-85-0; *p*-CH₃C₆H₄CO₂H, 99-94-5; *p*-CH₃COC₆H₄CO₂H, 586-89-0; *p*-CO₂HC₆H₄CO₂H, 100-21-0; CO₂, 124-38-9; C₆H₅OH, 108-95-2; C₆H₅Br, 108-86-1; *p*-CH₃C₆H₄I, 624-31-7; *p*-CH₃COC₆H₄Br, 99-90-1; (*p*-CH₃COC₆H₄)₂, 787-69-9; C₆H₅Pd^{II}(dppe), 60674-49-9.

One-Electron Oxidative Cleavage of Palladium(II) Alkyl and Phenoxo Bonds

Allen L. Seligson and William C. Troglor*

Contribution from the Department of Chemistry, 0506, University of California, San Diego, La Jolla, California 92093-0506. Received January 17, 1992

Abstract: One-electron oxidation of the d⁸ dialkyls Pd(CH₃)₂(dmpe), Pd[CH₂Si(CH₃)₃]₂(dmpe), and Pd(CH₃)[P(*t*-Bu)₂-(CH₂)₂CH(CH₂)₂P(*t*-Bu)₂], where dmpe = 1,2-bis(dimethylphosphino)ethane, by chemical or electrochemical methods results in homolytic cleavage of the Pd–alkyl bond to produce an alkyl radical and the corresponding cationic palladium(II) monoalkyl complex. In the presence of a trapping ligand, PPh₃, oxidation of Pd[CH₂Si(CH₃)₃]₂(dmpe) with [FeCp₂]PF₆, Cp = η-C₅H₅, produces Si(CH₃)₄ and [CH₂Si(CH₃)₃]₂ in a ratio similar to that obtained from the reaction between MgCl[CH₂Si(CH₃)₃] and [FeCp₂]PF₆. Because of the chemical irreversibility of the homolytic cleavage process, uphill electron transfer between Pd[CH₂Si(CH₃)₃]₂(dmpe) and electrochemically generated FeCp₂^{•+} could be observed with *k* = 46 ± 7 M⁻¹ s⁻¹ at 60 °C.

The oxidative cleavage reactions also exhibit selectivity. Oxidation of Pd(CH₃)[P(*t*-Bu)₂-(CH₂)₂CH(CH₂)₂P(*t*-Bu)₂] results in exclusive loss of the CH₃ group, and oxidation of Pd(CH₃)(OPh)(dmpe) results in preferential cleavage of the Pd–O bond. These results suggest the oxidative cleavage chemistry developed for d⁰ metal alkyls can be extended to late transition metals.

Introduction

Coordinatively unsaturated metal species act as highly reactive intermediates in hydrogenation, hydrosilylation, hydroformylation, and other reactions catalyzed by soluble transition metal complexes.¹ Mechanistic studies show that these complexes usually result from ligand dissociation or reductive elimination processes. Coordinative unsaturation has also been generated by photolysis, thermolysis, and electron transfer and with acidic, basic, or radical initiators.² Under the proper conditions stable complexes can be isolated.^{2,3} Jordan et al. have reported that the reaction

between Cp₂ZrR₂ and [Ag][BPh₄]⁴ or [Cp₂Fe][BPh₄]⁵ yields the [Cp₂ZrR]⁺ cation, which is an active ethylene polymerization catalyst. These highly reactive intermediate species are useful catalysts and often exhibit unique reactivity.^{2,3}

Previous research in our laboratory has explored the generation and subsequent reactivity of “Pt(PR₃)₂” and “Pd(PR₃)₂” coor-

(1) Parshall, G. W. *Homogeneous Catalysis. The Applications and Chemistry of Catalysis by Soluble Transition Metal Complexes*; John Wiley and Sons: New York, 1980.

(2) Collman, J. P.; Hegedus, L. S.; Norton, J. R.; Finke, R. G. *Principles and Applications of Organotransition Metal Chemistry*; University Science Books: Mill Valley, CA, 1987.

(3) (a) Jolly, P. W.; Jonas, K. *Agnew. Chem., Int. Ed. Engl.* 1968, 7, 731. (b) Englert, E.; Jolly, P. W.; Wilke, G. *Agnew. Chem.* 1971, 83, 84. (c) Linde, R.; Jongh, R. O. *J. Chem. Soc., Dalton Trans.* 1971, 563. (d) Fornies, J.; Green, M.; Spencer, J. L.; Stone, F. G. A. *J. Chem. Soc., Dalton Trans.* 1977, 1006. (e) Campion, B. K.; Heyn, R. H.; Tilley, T. D. *J. Chem. Soc., Chem. Commun.* 1988, 278. (f) Roddick, D. M.; Heyn, R. H.; Tilley, T. D. *Organometallics* 1989, 8, 324.

(4) Jordan, R. F.; Dasher, W. E.; Echols, S. F. *J. Am. Chem. Soc.* 1986, 108, 1718.

(5) Jordan, R. F.; LaPointe, R. E.; Bajgur, C. S.; Echols, S. F.; Willet, R. *J. Am. Chem. Soc.* 1987, 109, 4111.